

THE ROLE OF CRACK TIP CONSTRAINT FOR DUCTILE TEARING

W. Brocks* and W. Schmitt**

The quantities describing constraint and triaxiality and their relation with each other are discussed for various specimens and structures by comparison of numerical simulations of crack growth based on the J-integral concept and on micro-mechanical damage models with the corresponding experiments. It is shown that the "geometry dependency" of J_R -curves is a natural feature due to different patterns of plastic flow which, hence, cannot and should not be overcome by manipulating the definition of J. Instead, the dissipation of energy by plastic deformation explains the significant path dependency of J in steady state ductile crack growth.

INTRODUCTION

The influence of crack tip constraint and stress triaxiality on ductile fracture has been emphasized recently in explaining the geometry dependent resistance of specimens and structures to ductile tearing. As this is of major importance for the assessment of structural integrity by means of fracture mechanics concepts, it seems worthwhile to discuss the underlying idea and physical significance of "constraint".

Constraint is a structural feature which inhibits plastic flow and causes a higher triaxiality of stresses. It, therefore, may promote fracture, because the input of external work, e. g. measured by J, will to a lesser part be dissipated by plastic deformation but be available to enhance material degradation and damage. However, an engineering application of this concept requires a unique description of the quantities constraint, triaxiality, damage etc., allowing the quantitative evaluation of the involved parameters, e. g. by finite ele-

* Bundesanstalt für Materialforschung und -prüfung (BAM), Berlin
** Fraunhofer-Institut für Werkstoffmechanik, Freiburg

ment analyses. Though there is no doubt that the resistance against ductile tearing depends on the constraint or triaxiality of stresses (1 - 4), the problem still to be solved is how to define and quantify this parameter in a significant, reliable, and reproducible manner. Different definitions and measures are in use (5) and impede a comparison of various approaches to account for constraint.

Stress triaxiality is also known for promoting void growth on the micro-mechanical level (6, 7) and thus causing "damage" in the process zone. Constitutive equations which account for damage as e. g. Gurson's model (8) must, hence, be able to describe the physical effect of constraint on the tearing resistance as well. Both approaches will be used to describe the "geometry" effect on J_R -curves.

THE DUCTILE FAILURE PROCESS

Introducing substantial simplifications, the fracture process for most of the structural steels may take place either by the formation of microcracks and their coalescence, usually in an unstable manner (cleavage), or by the formation, growth, and coalescence of (micro)voids, usually in a stable manner (ductile).

In the case of brittle or cleavage fracture, only little plastic deformation is involved. The introduction of a critical cleavage stress made the quantitative description of these processes possible. With ductile fracture, significant amounts of plastic deformation are involved. Void formation takes place by decohesion of the particle-matrix interface, usually at non-metallic inclusions. With increasing stresses and strains, the voids grow larger until they reach a critical size when they coalesce, mainly by localized shear failure of the matrix between voids. A critical failure strain was proposed to describe the onset of failure.

Voids nucleate by decohesion of the particle-matrix interface at a critical radial stress or even by cracking of the particle. The growth of voids in a plastically deformed matrix (6, 7, 9) was investigated by several authors, all of whom found an exponential dependence of the growth rate on the stress triaxiality which is well in agreement with experimental observations. However, the size of voids calculated at the experimental failure load came out much smaller than expected. Coalescence process can, therefore, not be explained from the assumption of a homogenous strain field. Instead, localized (e. g. shear) deformation modes between voids must be considered in the final phase.

In terms of continuum mechanics, cracks cause singularities of the strain and/or stress fields. A measure of the singularities in the case of a nonlinear

elastic material is the J-integral. In combination with suitable material parameters, it may be used to describe the criticality of a crack.

In two-dimensional finite element analyses J may be computed directly from the contour integral since all quantities entering J are available. More efficient and easily extended to three-dimensional situations is the stiffness derivative method introduced by Parks (10).

Crack initiation and propagation are described by J-resistance curves. Although for materials described by incremental plasticity the evaluation of J becomes path-dependent with crack extension, the J-integral is still considered a valid fracture parameter for cases with limited amount of crack extension and, therefore, limited areas of non-proportional loading.

Lower constraint of a specimen apparently results in a steeper J_R -curve. Whether or not the value for crack growth initiation, J_i , does also depend on geometry effects, is still in dispute. A micro-mechanical model will, indeed, reveal an influence of constraint on J_i . It turns out, however, that J-resistance curves exhibit a pronounced dependence on specimen geometry (e. g. 11). This geometry dependence is explained by the fact that in the crack tip process zone different states of stress or "constraint" prevail in different specimen geometries. This influence of constraint may be taken into account on the basis of the J-integral concept by the introduction of constraint-modified resistance curves. This approach is confirmed by results obtained from micro-mechanical damage models (local approach) which assume a strong dependence of, e. g. the growth of cavities on the triaxiality of the stress field.

CONSTRAINT PARAMETERS

A common global measure is the plastic constraint factor, $L \geq 1$, defined by the ratio of the actual plastic collapse load of a flawed structure over the ideal plastic limit load of an unflawed body of the same net section, thus quantifying the restraint of plastic flow due to the presence of a flaw.

The local constraint at the crack tip may be measured by the ratio, d_n , of the load parameter, J, over the resulting characteristic deformation, δ , normalized by the yield stress, since less δ at a given J means more crack tip constraint (1). The linear relationship between J and δ can be derived from the HRR theory.

A physically significant definition of the resulting triaxiality of the stress state is simply given by the ratio, h, of the hydrostatic stress, σ_h , or first invariant of the stress tensor, which, in the classical theory of plasticity, does not cause any plastic deformation, over the von Mises equivalent stress, σ_e , which is the square root of the second invariant of the deviatoric stresses being responsible for plastic flow. This idea dates back to Hencky's diagram (12) of

effective shear stress, $\tau_r = \sigma_e/\sqrt{3}$, vs. hydrostatic stress. The physical meaning of this ratio was substantiated by the investigations of McClintock (6) and Rice and Tracey (7).

A few results are presented in the following which have been obtained by two-dimensional elastic-plastic finite element (FE) analyses. Plane strain condition was assumed as an appropriate model for side-grooved specimens. Thus, the following results refer to variations in the in-plane constraint, only. The analyses base on the incremental theory of plasticity by von Mises, Prandtl and Reuss in an updated Lagrangian formulation and simulate crack growth controlled by experimental J_R -curves (BAM), or by using the Gurson material model (Fh-IWM). Figs. 1a,b show the variation of σ_h/σ_e in the ligament ahead of the crack tip for a compact specimen (CT) and a centre cracked panel (CCT).

Different specimen geometries can be put in an order of constraint by any of these quantities, see (4) and Table 1. Generally, bend specimens like CT and SECB have a higher constraint than tensile specimens like CCT and SECT; thickness and/or side-grooving raise the constraint.

Advantages and drawbacks exist for each of the parameters:

- The global plastic constraint factor can be determined rather easily and reliably, even in experiments. But it is not suited to characterize the local variation of crack tip constraint in a structure.
- The local ratio d_n is strongly dependent on the hardening exponent, n , for high hardening which may even outweigh the discrimination between plane strain and plane stress. The definition of δ is conventionally restricted to a stationary crack and has to be extended for a growing crack.
- The range of values which the ratio h may take between the limiting cases of plane strain and plane stress is much wider than that of d_n , giving it a much better quantitative significance. But as the evaluation of h requires nonlinear FE calculations in any case, it will depend on the FE mesh and the solution strategy, more than CTOD and J do. In addition, the underlying stresses are usually subject to numerical oscillations along the crack front in three-dimensional problems.

Despite a general agreement among various authors (2 - 5) to use the ratio $h = \sigma_h/\sigma_e$ or its reciprocal as an appropriate measure of stress tri-axiality, there are still some unsolved problems. Unlike d_n , the ratio h is a local field quantity which varies not only with the crack front coordinate, z , but also with the distance to the crack front, r , and the ligament angle, θ . Hence, an additional assumption has to be made in order to decide which value is to be taken. This assumption is not only necessary to obtain reproducible numbers but will also be a question of physical importance. It may require the introduction of another material parameter, e. g. some critical length, L_c , over which h is measured.

A few proposals how to determine the stress triaxiality exist. HRR-theory and finite element (FE) analyses show that for mode I problems σ_h/σ_e has its maximum in the ligament, $\theta = 0$. Kordisch et al. (2) extrapolated $h(r)$ to the crack tip, $r \rightarrow 0$, from a small strain analysis whereas Brocks et al. (4, 14) used the maximum value ahead of the crack tip obtained from a geometrically nonlinear updated Lagrangian formulation. In a recent paper Clausmeyer et al. (5) took the slope $d(h^{-1})/dx$ to account for the shape of the curve in the ligament.

In the present paper the ratio of triaxiality, h_0 , has been calculated by a linear extrapolation to the crack tip, $(x - \Delta a) \rightarrow 0$, from an approximately linear branch of the $h(x)$ -curve. This rather arbitrary definition is used just because of numerical practicability as it avoids numerical oscillations near the maximum and the result, h_0 , does not depend so much on the FE mesh at the tip. Further studies are necessary before a physically meaningful definition of constraint or stress triaxiality seems possible.

THE PHYSICAL EFFECT OF CONSTRAINT ON DUCTILE CRACK GROWTH

Fig. 2a gives an example for the geometry dependency of J_R -curves (13). As the point of physical initiation is difficult to identify experimentally, little evidence on the geometry dependency of J_i exists. Commonly, J_i is supposed to be a material constant but there is some indication from R-curve testing contradictory to this assumption, see Table 1. It is not clear from a physical point of view, too, that triaxiality of the stress state should affect tearing resistance for $\Delta a > 0$ but not for $\Delta a = 0$. The slopes of the experimental R-curves, dJ/da , correlate with the triaxiality of the stress state, not only near initiation as has been shown before (2, 4), but also in the course of crack growth, see StE 460 results in Fig. 3b.

The dependency of J-resistance curves on the stress state is not only due to the fact that J as a loading parameter measures plastic work depending on the slip line pattern which develops out of the crack front and reaches the opposite free surface of the specimens when tested into the plastic collapse regime. Moreover, even the micro-mechanical processes of ductile tearing, namely void nucleation, growth, and coalescence depend strongly on the state of stress in the process zone.

Recently, a series of micro-mechanical models based on the concepts of continuum damage mechanics have been established to find alternatives. One of the new methods for ductile fracture analysis based on a yield condition by Gurson (8) has been developed and modified by Needleman, Tvergaard and others, e. g., (15). In this material model the plastic flow is influenced by microscopic voids which are represented by a single parameter, the void volume fraction, f . The basis for the modified Gurson model is a

plastic potential ϕ which is strongly dependent on the ratio of the hydrostatic stress over the von Mises equivalent stress, σ_h/σ_e .

For a steel ASTM A710, the material parameters for the Gurson model were derived from tension bars and used to predict the behaviour of a compact specimen CT25 with 20 % sidegrooves of the same material, yielding excellent agreement of the calculated and measured load vs. displacement curves and the respective J-resistance curves (16).

Although up to now, only two-dimensional simulations are feasible different specimen types were analyzed in order to evaluate relative differences of the predicted J-resistance behaviour which might be correlated to differences in the in-plane constraint. In the simulations, the meshing of the crack tip region and the critical distance L_c were kept constant. Among the geometries analyzed in (16), the results for the compact specimen and for the center cracked tension specimen are discussed here.

Fig. 2b shows the calculated J-resistance curves of these two specimens. Although the toughness level of the steel ASTM A710 is significantly higher than that of StE 460, the relative differences between the CT and the CCT specimens are similar. The variation of the in-plane constraint h over the ligament at initiation and after some amount of stable crack growth is very similar to that obtained for StE 460 (Fig. 1).

In each specimen the critical value of damage is reached at different levels of J. Thus, this model predicts geometry-dependent J_i -values as a consequence of differences in the crack tip constraint. Since the criterion for crack initiation must be reproducible, the initiation load is defined here as the load at which the first element (length 200 μm) on the ligament has reached the critical value of damage.

Fig. 3a compiles the calculated J_i -values (16) for all specimen geometries investigated as a function of the extrapolated values of stress triaxiality, h_0 , at initiation. There is a linear correlation between J_i and h_0 where lower constraint values correspond to higher J_i and vice versa. In Fig. 3b the slopes of the calculated resistance curves, dJ/da , are plotted as a function of h_0 , again taken at initiation. The slopes of the resistance curves were in every case determined between J_i and the J-value at a stable crack extension of 0.85 mm. As with the initiation values, a linear relation of dJ/da and h_0 may be deduced.

Also given in Fig. 3a are the initiation values obtained for StE 460. Here, the variation of J_i with h_0 is also present, but much less pronounced. In Fig. 3b the slopes of the resistance curves for the CT and CCT specimens of StE 460 are plotted vs. h_0 for initiation and for different amounts of crack extension. If only the situation at initiation is compared with the results for

ASTM A710, a very similar trend is observed. Even the development of the slope after initiation depends strongly on h_0 and may also be approximated by a linear function. The CT-specimen, however, does not show a variation of the slope with crack extension and increasing h_0 .

A linear function (dashed line) had also been postulated in (2) for a similar material and successfully applied to surface flaws. Recent results for a surface flaw in a pressure vessel (14) are also included in Fig. 3b. It is surprising that the curve determined from numerical simulations in plane strain of different specimen and loading conditions is fairly parallel to that derived only from smooth and sidegrooved compact specimens.

CONCLUSIONS

The influence of the state of stress in the process zone ahead of a crack front on initiation and ductile crack extension has been demonstrated for two different steels utilizing different experimental and numerical techniques including micro-mechanical damage models.

The appropriate quantitative assessment of constraint is possible by non-linear finite element analyses but depends on details of the numerical models. In order to make findings from different studies comparable, a pragmatical extrapolation scheme has been proposed to define a constraint parameter h_0 .

With increasing stress triaxiality h_0 , the slopes of the resistance curves decrease, within each material obviously in a self-similar way. The same trend has been found also for the initiation values J_i . Especially the experimental determination of crack initiation is extremely difficult and needs further investigations.

The dependence of initiation and slope of the resistance curve on constraint and, therefore, on geometry and size of the specimen or structure is an inherent feature of the ductile failure process. It is, in particular, supported by all available micro-mechanical failure models. This fact should, therefore, not be overruled by modifications of the J-integral.

The trends and dependencies found in several studies will facilitate the transferability of toughness values and resistance curves from laboratory specimens to real structures by taking into account the constraint in the specimen and in the structure.

REFERENCES

- (1) Steenkamp, P. A. J. M., "Investigation into the Validity of J-Based Methods for the Prediction of Ductile Tearing and Fracture", PhD Thesis, Technical University of Delft, 1986.
- (2) Kordisch, H., Sommer, E. and Schmitt, W., Nucl. Engng. and Design 112, 1989, pp. 27 - 35.
- (3) Aurich, D. and Sommer, E., Steel Research 59, 1988, pp. 358 - 367.
- (4) Brocks, W., Künecke, G. and Veith, H., "On the Influence of Triaxiality of the Stress State on Ductile Tearing Resistance", Proc. Symposium of Elastic-Plastic Fracture Mechanics: Elements of Defect Assessment, Freiburg, 1989.
- (5) Clausmeyer, H., Kußmaul, K. and Roos, E., Mat.-wiss. und Werkstoff-techn. 20, 1989, pp. 101 - 117.
- (6) McClintock, F. A., Trans. ASME, J. Appl. Mech. 35, 1968, pp. 363 - 371.
- (7) Rice, J. R. and Tracey, D. M., J. Mech. Phys. Solids 17, 1969, pp. 201 - 217.
- (8) Gurson, A. L., J. Engng. Mat. Tech. 99, 1977, pp. 2 - 15.
- (9) Budiansky, B., Hutchinson, J. W. and Slutsky, S., in: "Mechanics of Solids" (The Rodney Hill 60th Anniversary Volume). Edited by H. G. Hopkins and M. J. Sewell, Pergamon Press, Oxford, pp. 13 - 45.
- (10) Parks, D. M., Comp. Meth. Appl. Mech. Engng. 12, 1977, pp. 353 - 364.
- (11) Ernst, H. A., "Material Resistance and Instability beyond J-Controlled Crack Growth", in: "Elastic-Plastic Fracture", ASTM STP 803, 1983, pp. 191 - 213.
- (12) Hencky, H., Stahlbau 16, 1943, pp. 95 - 97.
- (13) Aurich, D., Wobst, K. and Krafka, H., Nucl. Engng. and Design 112, 1989, pp. 319 - 328.
- (14) Brocks, W., Künecke, G. and Wobst, K., Int. J. Pres. Ves. & Piping 39, 1989, pp. 77 - 90.

- (15) Needleman, A. and Tvergaard, V., J. Mech. Phys. Solids 35, 1987, pp. 151 - 183.
- (16) Sun, D.-Z. and Schmitt, W., "Application of Micromechanical Models to the Analysis of Ductile Fracture Resistance Behaviour", Proc. 5th Int. Conf. "Numerical Methods in Fracture Mechanics", Freiburg, 1990.

TABLE - Stable crack initiation and constraint.

specimen	B (B _N) [mm]	a/W [-]	J _i [N/mm]	L [-]	d _n [-]	h ₀ [-]
CT ¹⁾	25 (19)	0.58	117	1.58	1.88	2.6
CCT ¹⁾	20 (16)	0.49	127	1.16	1.30	1.1
CT ²⁾	25 (20)	0.62	218	-	-	2.73
CCT ²⁾	25 (20)	0.62	370	-	-	1.40

1) StE 460, R_{eL} = 460, R_m = 623 MPa
 2) A 710, R_{p0.2} = 619, R_m = 707 MPa

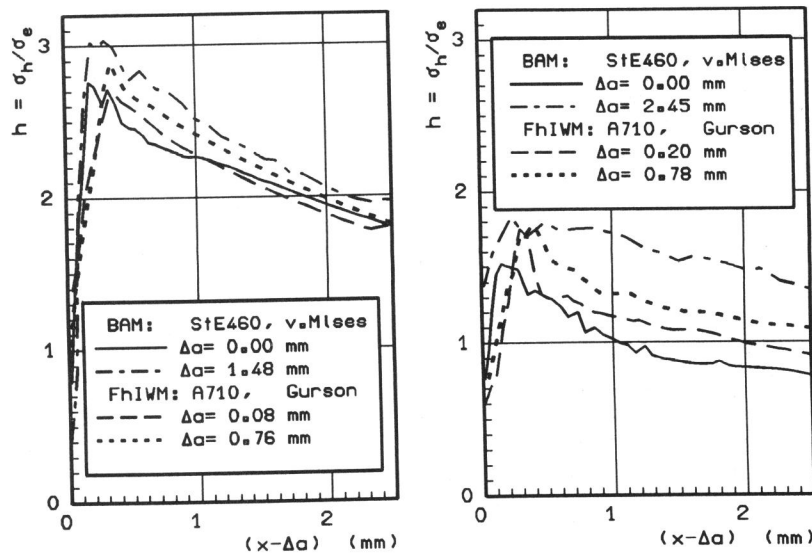


Fig. 1: triaxiality of the stress state in the ligament
 a) CT
 b) CCT

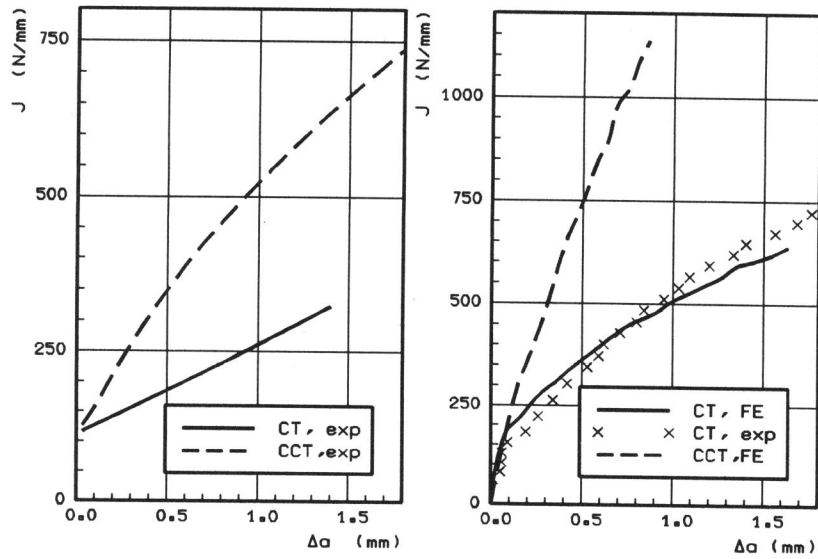


Fig 2: Geometry dependency of J-resistance curves
 a) StE460, BAM (13) b) A710, FhIWM (16)

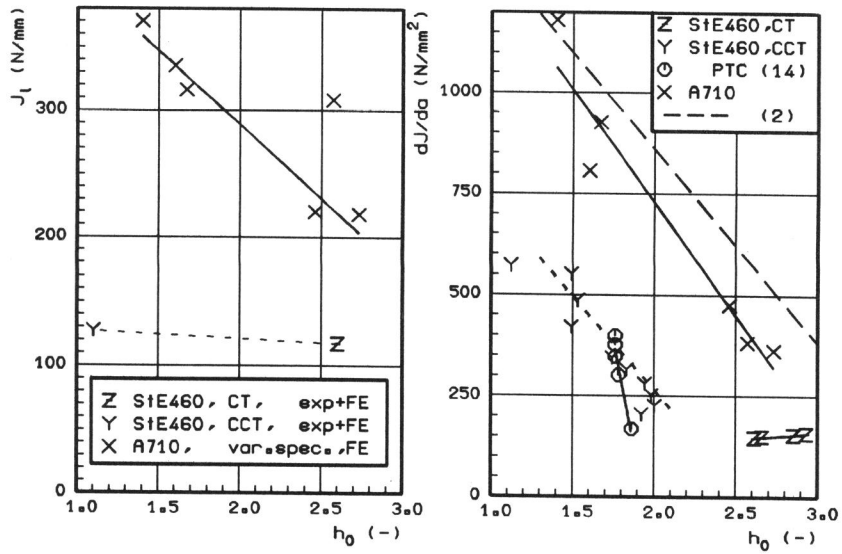


Fig 3: Irregularity and tearing resistance
 a) Initiation (Table 1) b) slope